Catalysis Science & Technology

Accepted Manuscript

ROYAL SOCIETY OF CHEMISTRY

www.rsc.org/catalysis

Catalysis Science & Technology RSCPublishing

ARTICLE

Synthesis of ethyl hexyl ether over acidic ion-exchange resins for cleaner diesel fuel

Cite this: DOI: 10.1039/xoxxoooooox

J.Guilera, E. Ramírez, C. Fité, J. Tejero* and F. Cunill

Received ooth January 2012,
Accepted ooth January 2012

DOI: 10.1039/xoxxoooooox

www.rsc.org/

The synthesis of ethyl hexyl ether as suitable diesel additive was investigated using 1-hexanol and diethyl carbonate as reactants and acidic ion-exchange resins as catalysts. Liquid-phase experiments were performed in a batch reactor at the temperature range of 403-463 K and 2.5 MPa. The formation of ethyl hexyl ether proceeded from two routes: thermal decomposition of ethyl hexyl carbonate and intermolecular dehydration of 1-hexanol with ethanol. Both pathways require the previous transesterification reaction between diethyl carbonate and 1-hexanol. It was revealed that this reaction is favoured in polymer zones of 0.4 nm/nm^3 of polymer density (equivalent to 2.6 nm diameter pores in inorganic materials). Acidic ion-exchange resins containing a significant volume fraction of this polymer density are Dowex 50Wx2 and Amberlyst 70. By using this kind of catalyst, reaction rate and selectivity are significantly increased. Finally, it was observed that working at low temperature would favour the selectivity to ethyl hexyl carbonate and hinder the undesired formation of alkenes.

1. Introduction

Complete combustion of diesel fuel only produces carbon dioxide and water but actual combustion in diesel engines is incomplete and forms toxic air contaminants. In particular, diesel vehicles are the largest worldwide contributors to particulate matter pollution in urban areas, where most people live. Compared to similar-sized gasoline engines, diesel combustion generates about 100-fold more particles for travelled distance. These particles form deposits in lungs with what an increased risk of premature mortality ensues[1-4]. Far from be undervalued, Yim and Barret estimated that road pollution in UK is twice as deadly as traffic accidents[5].

A feasible technical solution able to reduce the amount of particulates in diesel exhaust, with little or no penalty on nitrogen oxide emissions, is the use of diesel blends containing oxygenated compounds, commercially known as oxygenated diesel[6-9]. Traditional oxygenates used in gasoline formulation are unsuitable for incorporation into diesel fuel blends due to their low cetane numbers, leading to diminished fuel performance. In contrast to the branched ethers currently used in gasoline blends (e.g. methyl and ethyl tert-butyl ether), linear ethers are preferred in the case of diesel fuel for cleaner fuel burning purposes[10-12].

Among linear ethers, some attention has been focused on ethers containing ethyl groups as the origin of the ethyl group can be renewable bioethanol[13-17]. Ethyl ethers can be synthesized directly from the dehydration reaction of two ethanol molecules, or else, by the reaction between ethanol with a longer alcohol. From an industrial perspective, both options have their pros and cons, and actually they are perfectly compatible. The first option forms diethyl ether, which is the more economical ethyl ether compound, but as a result of its low flash point, it changes considerably the initial diesel properties. Thus, the addition of large quantities of diethyl ether to diesel should be avoided. A second option, more expensive due to the lower availability of longer alcohols, forms asymmetrical linear ethers with excellent properties as diesel fuels. As a result, it is not necessary to restrict their addition from a technical standpoint but it should be optimized from an economical one. Ethyl hexyl ether is an ethyl ether of the latter group that provides a good compromise between blending cetane number and cold flow properties[18,19].

Literature dealing with ethyl hexyl ether synthesis is scarce. However, on the analogy of similar ether syntheses, there are several potential organic routes able to produce industrial amounts of ethyl hexyl ether, all consisting in the ethylation of 1-hexanol. Three cost-effective ethylating agents showed interesting performances in analogous reactions: ethanol, diethyl carbonate and diethyl ether. Among these three environmentally benign ethylating agents, diethyl carbonate is the most reactive one and gives rise to successful conversion at lower temperature[20-22].

The chance of decreasing the reaction temperature in the formation of ethyl hexyl ether is especially relevant to hinder alkene formation, in the present case C_6 alkenes[23]. The formation of alkenes, by means of intramolecular dehydration of an alcohol (reactant) or via cracking of ether (product), has higher dependency with the temperature than the desired production of ethers. In this sense, at temperatures above 523 K the undesired formation of alkenes becomes the dominant

Chemical Engineering Department, Faculty of Chemistry, University of Barcelona, c/Martí i Franquès 1, 08028 Barcelona, Spain.
E-mail: jtejero@ub.edu

process[20,24,25]. Therefore, reactor temperature should be kept below 523 K. At this relatively low temperature, acidic ion-exchange resins are interesting candidates to be used as catalysts because they exhibit higher concentration of acid sites (≈ 5 mmol H^+/g) compared to most other solid acids. Thus, even the strength of the resin acid sites tend to be lower than those found on zeolites and similar solid acids, they are typically more active at lower temperatures[26-29]. In this line, the production of the ethers used in gasoline blends is nowadays carried out on acidic ion-exchange resins at industrial scale.

Catalytic performance of different types of acidic ion-exchange resins can be extremely different because of the exchange capacity of acidic resins is chiefly conditioned by their molecular accessibility, namely, by their ability to be crossed by reactants and products moving to and from the active sites. On these grounds, it appears quite obvious that any application of acidic ion-exchange resins ought to be preceded by a careful examination of the resin morphology[30-34].

Morphology of polymeric resins cannot be well characterized by conventional porosimetry methods as mercury intrusion or nitrogen adsorption-desorption since they require completely dry samples. Using such data to interpret the different performances observed (e.g. in reactions carried out in solvents) requires the assumption that the resin morphology is not significantly changed when it is wetted with solvent. This assumption is clearly not valid using hydrophilic polymeric catalysts in liquid-phase polar reaction environments[31].

Therefore, other characterization techniques are needed in order to study the actual morphology of acidic ion-exchange resins in the reaction media. To the best of our knowledge, the only procedure employed to assess the morphology of ion-exchange resins in a swollen state has been the Inverse Steric Exclusion Chromatography (ISEC) technique

Previous works revealed that most catalytic performances can be qualitatively predicted by the morphological description in swollen-state given by ISEC technique[18,27,34,35]. The aim of this work is to study the synthesis of ethyl hexyl ether from 1-hexanol and diethyl carbonate over acidic ion-exchange resins (Fig. 1). In this sense, catalytic performances are evaluated and relationships between ISEC data of catalysts and their catalytic behaviour are obtained. The effect of the temperature on the reaction system is also studied.

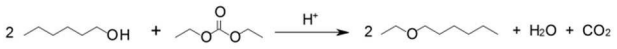

Fig. 1 Target reaction of this work.

2. Experimental

2.1 Materials

1-hexanol (≥98%, Acros) and diethyl carbonate (≥99%, Acros) were used as reactants. Distilled water, ethanol (≥99%, Panreac), 1-hexene (≥99%, Aldrich), di-n-hexyl ether (≥97%, Fluka) and ethyl hexyl ether (≥99%, produced and purified by rectification in our lab) were used for analysis purposes. N_2 was used to pressurize the reactor (≥ 99.995%, Abelló Linde) and He as chromatographic carrier gas (≥ 99.998%, Linde).

Nine commercial acidic ion-exchange resins based on a styrene-co-divinylbenzene polymer, supplied by Rohm and Haas France (Amberlyst 15, 16, 39, 46 and 70), Aldrich (Dowex 50Wx8, 50Wx4 and 50Wx2) and Purolite (Purolite CT482), were used as catalysts. As Table 1 shows, tested resins cover a wide range of structural properties and acid capacities, with the goal of evaluating their influence on the catalysts activity. Over-sulfonated resins were not used since they hardly increased the catalytic performances in similar reactions[18,34], while the over-sulfonation procedure supposes an increase of manufacturing cost.

2.2 Characterization of ion-exchange resins

Morphology of ion-exchangers in swollen-state was analysed from inverse steric exclusion chromatography (ISEC). ISEC apparatus consisted of HPLC pump (Waters 510), sampling valve, stainless steel column (4.27 cm^3) and refractometric detector (Shodex RI-100). The detector signal was connected to a computer and the sampling data was synchronized with the mobile phase flow rate using a drop counter

Catalysts were crushed, sieved in swollen state ($0.125 \leq d_p \leq 0.250$ mm) and placed overnight in the mobile phase (a 0.2N solution of Na_2SO_4 in aqueous phase measurements). Then, the swollen catalyst was packed in the column by flowing the mobile phase for 30 min (≈ 5 mL/min), and connected to the apparatus. During chromatographic measurements, the standard

Table 1. Specific characteristics of used ion-exchange resins[27,34].

Structure		Acid capacity (mmol H^+/g)[a]		
	DVB (%)	High[b]	Medium[c]	Low[d]
		[4.80-4.95]	[2.65-4.25]	[0.87]
Macroreticular	20	Amberlyst 15		Amberlyst 46
	12	Amberlyst 16	Purolite CT482	
	8	Amberlyst 39	Amberlyst 70	
Gel-type	8	Dowex 50Wx8		
	4	Dowex 50Wx4		
	2	Dowex 50Wx2		

[a]Titration against standard base. [b]Conventionally sulfonated, with stoichiometric amount of sulfonic groups: a sulfonic group by styrene ring. [c]Conventionally sulfonated chlorinated resins. [d]Surface sulfonated: sulfonation restricted to external gel-phase layers.

Catalysis Science & Technology RSCPublishing

ARTICLE

solutes of known molecular sizes (deuterium oxide, sugars and dextrans) were injected independently (20 µL). Elution volumes were determined on the basis of the first statistical moments of the chromatographic peaks. For each solute the measurement was repeated three times for determination of the experimental error. At the end of the measurements, the catalyst was washed with distilled water, quantitatively extruded from the column, dried overnight (T = 383 K), and finally weighted

Acid capacity was measured by titration against standard base.

2.3 Experimental set-up

Experiments were conducted in a 100-mL stainless steel autoclave which operates in batch mode. A magnetic drive turbine was the mixing system and an electric furnace was the heating one (±1 K). One of the reactor outlets was connected directly to a liquid sampling valve, which injected 0.2 µL of pressured liquid into a gas-liquid chromatograph (HP6890A, Hewlett Packard) equipped with a thermal conductivity detector. A 50 m x 0.2 mm x 0.5 µm methyl silicone capillary column was used to determine the composition of liquid mixtures. The column was temperature programmed to start at 323 K with a 10 K/min ramp to reach 573 K and held for 6 min. He flow rate was set at 30 mL/min. All the species were identified by a second chromatograph equipped with a mass spectrometer (GC/MS 5973, Agilent).

2.4 Procedure

Catalysts were dried at room temperature for 24 h prior to mechanical sieving ($0.40 \leq d_p \leq 0.63$ mm). After sieving, resin samples were dried at 383 K, firstly at atmospheric pressure during 3 h and, subsequently, under vacuum overnight. This drying procedure assures a water content of resins of less than 3 wt. %[34].

The reactor was filled with 70 mL of a mixture of 1-hexanol and diethyl carbonate (molar ratio $R_{HeOH/DEC} = 2$). Then, the liquid was heated up to the working temperature and stirred at 500 rpm. The pressure was kept at 2.5 MPa with N_2 ensuring that the reaction medium was in the liquid-phase. At those conditions, the gas phase was composed by N_2 and carbon dioxide, the only non-condensable product. The change volume of the liquid phase by the CO_2 exit to the gas phase was partially neutralised by the change of density of the liquid phase so that no change in the volume of the liquid phase was observed. When the mixture reached the working temperature (approximately after 15 minutes), the dry catalyst was injected into the reactor from an external cylinder by a N_2 pulse. Experiments were carried out in the temperature range 403-463 K. The amount of used catalyst was changed at each temperature within the range 0.2-3.7 g in order to obtain similar conversion levels during the whole series of experiments performed over each single catalyst.

Catalyst injection was taken as the time zero. At that moment, no conversion of 1-hexanol was observed but conversion level of diethyl carbonate, which suffers thermal decomposition, was always less than 1%. The composition of the liquid mixture was analysed hourly until the end of the experiment (6 h) to obtain the mole variation over time for all species. All the catalytic tests were, at least, replicated once to assure the data reproducibility. Experimental error shown in this work corresponds to standard deviation between replicated experiments.

In each experiment, conversion of reactant *j* (X_j), selectivity (S_j^k) and yield (Y_j^k) to product *k* with respect to reactant *j* were calculated by:

$$X_j = \frac{\text{moles of j reacted}}{\text{initial moles of j}} \times 100 \ [\%] \quad (1)$$

$$S_j^k = \frac{\text{moles of j reacted to form k}}{\text{moles of j reacted}} \times 100 \ [\%] \quad (2)$$

$$Y_j^k = \frac{\text{moles of j reacted to form k}}{\text{initial moles of j}} \times 100 \ [\%] \quad (3)$$

Initial reaction rates of formation of compound *j* (r_j^0) were found from the slope of curves of number of moles of compound *j* (n_j) versus time, were W_{cat} is the mass of dry catalyst:

$$r_j^0 = \frac{1}{W_{cat}} \left(\frac{dn_j}{dt}\right)_{t=0} \left[\frac{mol}{h \cdot kg_{cat}}\right] \quad (4)$$

At the selected reaction conditions (temperature, pressure, stirring speed, particle size and catalyst mass), it is assumed that the obtained reaction rates were not influenced by mass transfer effects on this reaction set-up[23,27,36].

3. Results

3.1 Morphology of ion-exchange resins

Ion exchange resins swell in liquid polar media, particularly in aqueous phase, and non-permanent pores between polymer chains (spaces) appear. A description of resins morphology in swollen state can be obtained by analysis of ISEC data. Porous structure is modelled as a set of discrete volume fractions each composed of pores having simple geometry and uniform sizes. A portion of open spaces in macromolecular resins can be characterized by the cylindrical pore model ("true pores"). The true pore diameter ranged in the 10-118 nm zone in Amberlyst 15 and 16, and in the 8-41 nm zone in Amberlyst 39 and 70, and Purolite CT482; most of such spaces lying in the 8-10 nm zone. Swollen gel-type resins do not show spaces in the range of mesopores.

Cylindrical pore model is unable to describe the spaces between polymer chains formed in the micropore range. A good view of the three-dimensional polymer network of swollen gel-phase is given by the Ogston geometrical model, in which micropores are described by spaces between randomly oriented rigid rods[37]. From ISEC data, the Ogston model makes possible to estimate the specific volume of swollen polymer (free space plus that occupied by the skeleton), V_{sp}, and also to distinguish gel zones of different density or polymer chain concentration. Gel-phase porosity is described as a set of zones of different chain density. According to the Ogston model, the pore size of each gel-phase zone is represented as the total length of polymer chains per unit of volume of swollen polymer (nm/nm^3 or nm^{-2})[35,38-42].

Catalysis Science & Technology RSCPublishing

ARTICLE

Table 2. Morphology of the polymer gel-phase swollen in water, acid capacity and maximum operation temperature of catalysts

Catalyst / Polymer fraction density [nm/nm^3]	V_{sp} (cm^3/g)[a]						Acid capacity (mmol H$^+$/g)[b]	T_{max} (K)[c]
	0.1	0.2	0.4	0.8	1.5	Total		
Amberlyst 15					0.622	0.622	4.81	393
Amberlyst 16	0.208			0.016	0.913	1.136	4.80	393
Amberlyst 39	0.218		0.588	0.243	0.595	1.643	5.00	403
Amberlyst 46	0.010			0.016	0.164	0.190	0.87	423
Amberlyst 70	0.071	0.007	1.072			1.149	2.65	463
Purolite CT482			0.093	0.249	0.740	1.081	4.25	463
Dowex 50Wx2		0.729	1.949			2.677	4.83	423
Dowex 50Wx4			0.639	1.281		1.920	4.95	423
Dowex 50Wx8		0.034		0.046	1.325	1.404	4.83	423

[a] ISEC method. [b]Titration against standard base. [c]Manufacturer data

In particular, the specific volume of swollen polymer (V_{sp}) has been modelled in 5 zones of polymer chains concentration of 0.1, 0.2, 0.4, 0.8 and 1.5 nm/nm^3; the sum of estimated volumes of the swollen gel fractions used is the total V_{sp} value. The spaces between chains in such zones are equivalent to pore diameters of 9.8, 4.3, 2.6, 1.5 and 1 nm, respectively[43,44]. Table 2 shows gel-phase morphology data of tested catalyst in swollen state. As seen, V_{sp} decrease on macroreticular and gel-type resins and, accordingly, predominant gel-phase is denser, on increasing DVB%. The densest resins in swollen state are Amberlyst 15 and 16 and Dowex 50Wx8 which show chain concentrations of 1.5 nm^{-2}, and less dense ones are Dowex 50Wx2 with polymer density in the range 0.2-0.4 nm^{-2} and Amberlyst 70 (0.4 nm^{-2}). Dowex 50Wx4 (0.4-0.8 nm^{-2}), Amberlyst 39 (0.4-1.5) and Purolite CT482 (0.8-1.5 nm^{-2}) show intermediate density values

Table 2 also shows the acid capacity and the maximum operation temperature recommended from the manufacturers of tested ion-exchange resins.

3.2 Reaction network

Fig. 2 shows the evolution of the number of moles of each compound over time in an experiment conducted on Dowex 50Wx2, which can be taken as representative of the whole series of experiments. As shown, the consumption-rate of both reactants followed the same pattern (see Fig. 2A). Thus, it can be inferred that the reactivity of diethyl carbonate and 1-hexanol on acidic ion-exchange resins is quite similar. The number of 1-hexanol moles present in the liquid-phase was always higher than that of diethyl carbonate since the alcohol was initially in excess.

From the very beginning, reactants were consumed leading to the formation to several compounds. Ethyl hexyl carbonate, ethanol, ethyl hexyl ether, di-n-hexyl ether and diethyl ether were always formed in significant amounts; water and di-hexyl carbonate were formed in much lower quantities (not plotted for the sake of clarity) and C_6 alkenes were only detected on some ion-exchange resins.

The reaction products can be divided into two groups depending on their evolution pattern. On one hand, ethyl hexyl carbonate and ethanol showed the typical behaviour of reaction intermediate compounds in a batch-type experiment (see Fig. 2B). Their number of moles was highly increased during the first hours of reaction, and subsequently, they showed a plateau in the case of ethanol and a slight maximum in the case of ethyl hexyl carbonate. This behaviour suggests that they were firstly produced in one reaction and then consumed in a second one, pointing out that those compounds take part in some reactions in series. On the other hand, the number of moles of the three ethers formed, ethyl hexyl ether, di-n-hexyl ether and diethyl ether, keeps increasing until the end of the experiment (see Fig. 2C). As a result, conversion of reactants, selectivity and yield to ethyl hexyl ether (see Fig. 3A, 3B and 3C, respectively), as well as yield to other ethers, steadily increase during the whole experiment. Therefore, it is clear that for industrial purposes, longer contact times are necessary.

The observed distribution of products suggests the reaction network shown in Fig. 4. As seen, several plausible reactions are involved forming a series-parallel scheme. According to the proposed scheme, the synthesis of ethyl hexyl ether proceeds from two simultaneous reaction pathways. The first one forms ethyl hexyl ether and carbon dioxide, involving transesterification reaction of diethyl carbonate to ethyl hexyl carbonate and ethanol (reaction 1) and thermal decomposition of the ethyl hexyl carbonate (reaction 2). The second one forms ethyl hexyl ether and water, involving reaction 1 and intermolecular dehydration of ethanol with 1-hexanol (reaction 3).

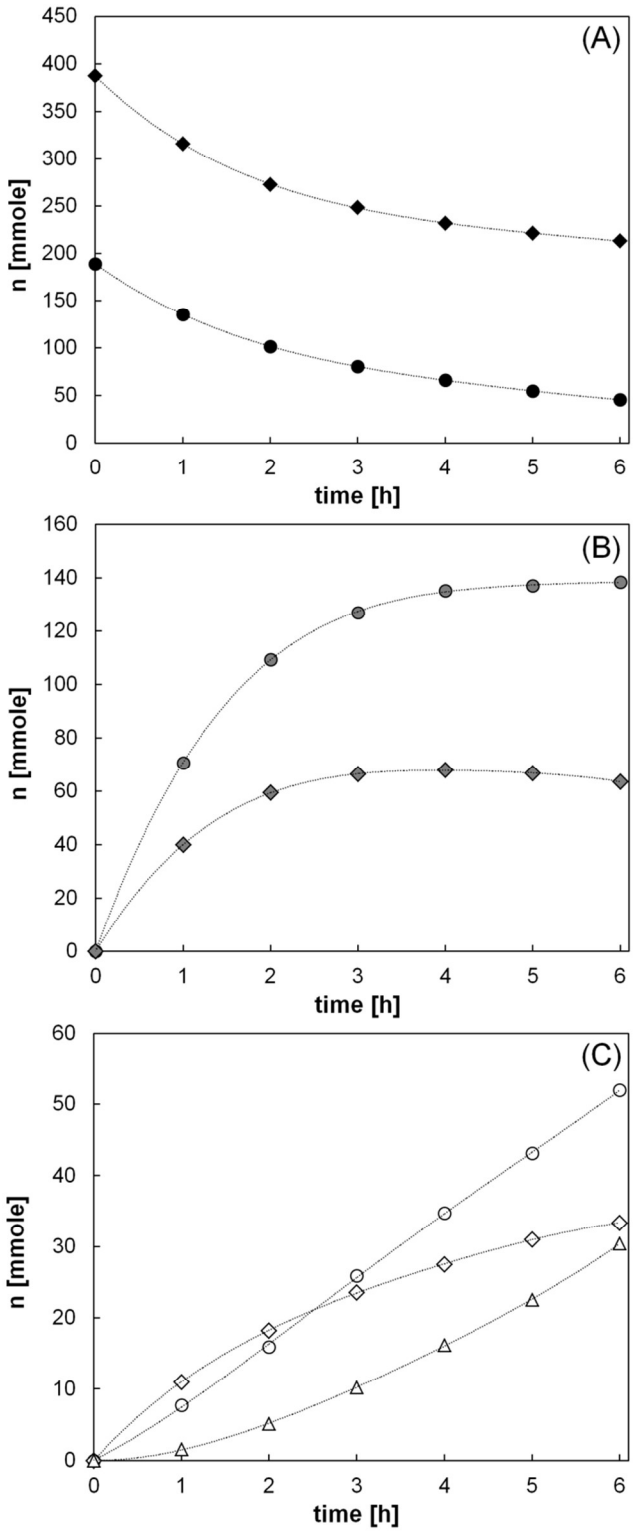

Fig. 2 Evolution of the mole number of species over time, A (♦ 1-hexanol; ● diethyl carbonate), B (● ethanol; ♦ ethyl hexyl carbonate), C (○ ethyl hexyl ether; ◊ di-n-hexyl ether; Δ diethyl ether). Experimental conditions: T=423 K, P=2.5 MPa, W_{cat}=1 g, $R_{HeOH/DEC}$=2, catalyst Dowex 50Wx2.

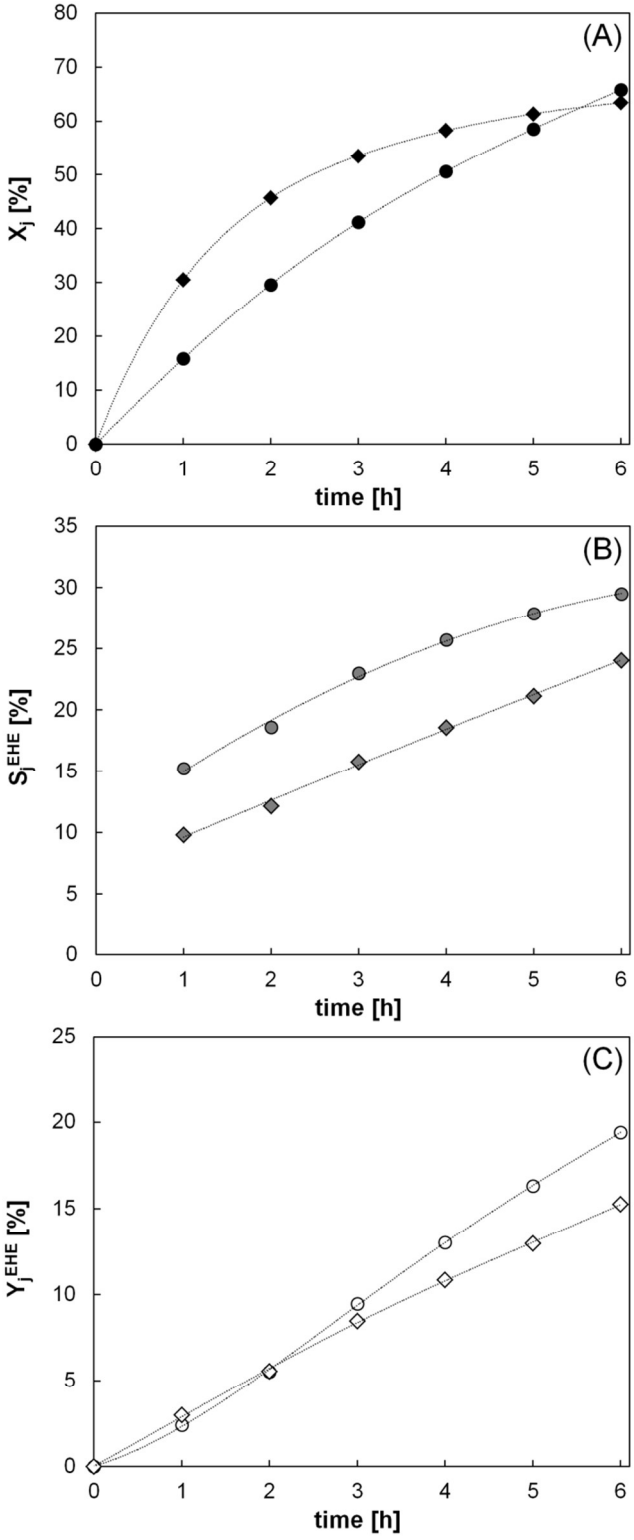

Fig. 3 Evolution of the reactant conversion (A), selectivity (B) and yield to ethyl hexyl ether (C) over time. Compound *j*: diethyl carbonate (round circles), 1-hexanol (diamonds). Experimental conditions T=423 K, P=2.5 MPa, W_{cat}=1 g, $R_{HeOH/DEC}$=2, catalyst Dowex 50Wx2.

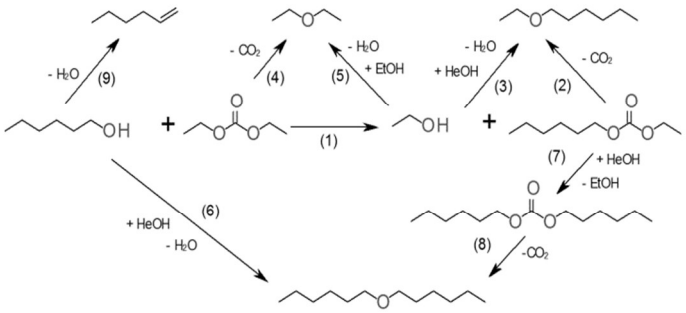

Fig. 4 Series-parallel reaction scheme between 1-hexanol and diethyl carbonate over acidic ion-exchange resins.

Altogether, they form two moles of ethyl hexyl ether, one of carbon dioxide and one of water by consuming two moles of 1-hexanol and one of diethyl carbonate (see target reaction, Fig. 1). Reaction 1 takes place in both pathways and thereby it is mandatory step for the further formation of ethyl hexyl ether.

The routes of diethyl ether and di-n-hexyl ether formation are analogous to that of ethyl hexyl ether (reactions 4-5 and 6-8, respectively). Moreover, small amounts of C_6 alkenes were formed from the intramolecular dehydration of 1-hexanol on some resins (reaction 9). For simplicity, the nine reactions can be grouped into four different kinds of reactions:

(i) transesterification of carbonates (reactions 1 and 7),
(ii) thermal decomposition of carbonates (reactions 2, 4 and 8)
(iii) alcohol intermolecular dehydration (reactions 3, 5 and 6)
(iv) alcohol intramolecular dehydration (reaction 9).

3.3 Catalyst screening

Data obtained for all tested catalysts are summarized in Table 3. After 6h of reaction, conversion of diethyl carbonate ranged 12-66% and that of 1-hexanol ranged 24-63%. As a rule, similar level of conversion was achieved from both reactants, 1-hexanol being slightly more reactive than diethyl carbonate. These results highly differ from those obtained in a previous work when 1-octanol was used instead of 1-hexanol for obtaining ethyl octyl ether[34]. In that case, diethyl carbonate was much more reactive than the alcohol and the formation of diethyl ether was more favoured than ethyl octyl ether synthesis. In the present reaction, the higher reactivity of 1-hexanol contributes positively to the formation of the asymmetrical ether.

As above mentioned, yields obtained were rather low for industrial purposes; they ranged 2-19% with respect to diethyl carbonate and 3-16% with respect to 1-hexanol. Nevertheless, the significant amount of intermediate products still present at the end of the run (Fig. 3B) and the continuous increase of the yield with time (Fig. 3C), indicate that higher amounts of ethyl hexyl ether can be easily achieved by increasing contact time and/or the reaction temperature.

Among tested catalysts, the most active in terms of reactants conversion and yield to ethyl hexyl ether was Dowex 50Wx2 (X_j=63-66% and Y_j^{EHE}=15-19%). Even though this low crosslinked gel-type resin was initially designed for fine chemical and pharmaceutical column separation purposes, lately it has shown satisfactory catalytic performance in several types of reactions; *e.g.* bio-oil upgrading, glycerol acetylation, dehydration of alcohols and synthesis of glycol and bisphenol A[45-48]. Besides, it has been reported as suitable support for embedding Ru nanoparticles as bifunctional catalyst for γ-valerolactone formation[49]. The high capacity of Dowex 50Wx2 to swell the polymer backbone in the polar medium due to low divinylbenzene content was found to be crucial for accessing the inner sulfonic acid sites.

Table 3. Conversion of reactants and yield to ethyl hexyl ether (T=423 K, P=2.5 MPa, W_{cat}=1 g, $R_{HeOH/DEC}$=2, t=6h).

	X_{DEC} (%)	X_{HeOH} (%)	Y_{DEC}^{EHE}(%)	Y_{HeOH}^{EHE} (%)
Amberlyst 15	32.2 ± 0.5	44.1 ± 0.4	10.1 ± 0.1	10.2 ± 0.1
Amberlyst 16	41.8 ± 0.2	52.2 ± 0.5	13.8 ± 0.1	13.1 ± 0.1
Amberlyst 39	54.8 ± 1.5	58.4 ± 1.5	17.2 ± 0.5	14.6 ± 0.1
Amberlyst 46	11.7 ± 0.9	24.0 ± 1.2	2.1 ± 0.5	2.7 ± 0.6
Amberlyst 70	44.8 ± 0.8	56.6 ± 0.2	12.6 ± 0.7	10.7 ± 0.5
Purolite CT482	53.9 ± 1.8	57.8 ± 0.2	17.3 ± 0.6	15.1 ± 0.8
Dowex 50Wx2	65.9 ± 0.1	63.4 ± 0.2	19.4 ± 0.1	15.3 ± 0.1
Dowex 50Wx4	61.1 ± 1.6	61.2 ± 1.2	19.1 ± 1.5	15.5 ± 0.8
Dowex 50Wx8	48.6 ± 0.5	56.7 ± 0.2	15.7 ± 0.1	13.9 ± 0.1

Amberlyst 46 was the less active catalyst for obtaining ethyl hexyl ether (X_j=12-24% and Y_j^{EHE}=2-3%). A special property of Amberlyst 46 is the small amount of sulfonic groups within the gel-phase because the sulfonation is restricted to only the first few layers of styrene rings. Considering the low catalytic activity shown by Amberlyst 46, it can be assured that the presence of sulfonic groups located within the gel-phase clearly promotes the formation of ethyl hexyl ether. However, as several reactions are involved in this catalytic process, special attention has to be paid on the selectivity within the gel-phase.

As most series-parallel reaction systems, the selectivity was clearly influenced by the conversion level, in such a way that the selectivity to ethyl hexyl ether increased with reactants conversion (see Fig. 3B). For comparison purposes, Table 4 shows selectivity data at the same level of diethyl carbonate conversion (X_{DEC}=10%), estimated from the mole-time curves. That conversion level was reached with all catalysts in less than 2 hours of reaction, but with Amberlyst 46 more than 5 hours were necessary to achieve it. At this initial stage of reaction, it has been assumed that all the products were formed directly from reactants. Thus, diethyl carbonate should only form ethyl hexyl carbonate by the transesterification with 1-hexanol (reaction 1) or it can be thermally decomposed to diethyl ether (reaction 4); and analogously 1-hexanol should only form ethylhexyl carbonate (reaction 1), react with another 1-hexanol molecule giving place to di-n-hexyl ether (reaction 6) or form C_6 alkenes by dehydration (reaction 9). With this approach, the reaction network at the initial reaction time was simplified from nine series-parallel reactions to four parallel ones

In general, diethyl carbonate reacted readily with 1-hexanol and interesting selectivities to ethyl hexyl carbonate were achieved (84 % < S_{DEC}^{EHC} < 98%), what indicates that the loss of ethyl groups to diethyl ether formation was certainly hindered on some catalysts (2% < S_{DEC}^{DEE} <16%). On the contrary, the ability of 1-hexanol to react with diethyl carbonate is significantly lower (44% < S_{HeOH}^{EHC} <72%), mainly because such reaction competes with the di-n-hexyl ether formation by the dehydration reaction of two hexanol molecules

Catalysis Science & Technology RSCPublishing

ARTICLE

Table 4. Estimated selectivity at the conversion level of X_{DEC}=10% (T=423 K, P=2.5 MPa, W_{cat}=1 g, $R_{HeOH/DEC}$=2).

	time (min)	X_{HeOH} (%)	S^{EHC}_{DEC} (%)	S^{DEE}_{DEC} (%)	S^{EHC}_{HeOH} (%)	S^{DHE}_{HeOH} (%)	$S^{alkenes}_{HeOH}$ (%)
Amberlyst 15	123 ± 2	24.5 ± 0.1	84.4 ± 2.4	15.6 ± 2.4	43.8 ± 1.1	39.4 ± 1.2	16.9 ± 1.1
Amberlyst 16	89 ± 1	25.5 ± 1.0	89.2 ± 0.8	10.8 ± 0.8	49.1 ± 1.3	43.8 ± 1.4	7.1 ± 1.7
Amberlyst 39	61 ± 3	22.1 ± 1.0	95.2 ± 1.6	4.8 ± 1.6	59.3 ± 2.0	39.0 ± 0.7	2.2 ± 2.0
Amberlyst 46	311 ± 24	21.2 ± 0.2	97.6 ± 1.6	2.4 ± 1.6	68.9 ± 1.6	30.0 ± 0.7	1.1 ± 0.7
Amberlyst 70	70 ± 1	22.6 ± 0.4	96.2 ± 2.4	3.8 ± 2.4	64.6 ± 1.2	35.7 ± 0.5	0.6 ± 0.6
Purolite CT482	64 ± 1	22.6 ± 0.4	91.6 ± 1.4	8.4 ± 1.4	54.6 ± 1.4	42.1 ± 0.6	3.3 ± 1.8
Dowex 50Wx2	37 ± 1	19.8 ± 0.1	96.3 ± 0.7	3.7 ± 0.7	72.4 ± 0.5	27.6 ± 0.4	0.0 ± 0.0
Dowex 50Wx4	47 ± 1	20.9 ± 0.6	95.0 ± 1.2	5.0 ± 1.2	67.0 ± 1.3	33.2 ± 1.4	0.1 ± 0.1
Dowex 50Wx8	71 ± 1	24.3 ± 0.3	93.1 ± 2.1	6.9 ± 2.1	52.0 ± 0.7	44.6 ± 1.3	3.4 ± 1.2

($28\% < S^{DHE}_{HeOH} < 45\%$). Finally, it is observed that the formation of C_6 alkenes via intramolecular dehydration of 1-hexanol is hardly significant on some particular catalysts ($0\ \% < S^{alkenes}_{HeOH} < 17\%$). In summary, the dehydration of two molecules of 1-hexanol to give di-n-hexyl ether and water is the main competitive reaction of the desired reaction between diethyl carbonate and 1-hexanol, necessary step for the further formation of ethyl hexyl ether.

From all the data collected, it is seen that Dowex 50Wx2 is the most active catalyst, and also the most selective to form ethyl hexyl carbonate. Interestingly, Dowex 50Wx2 (fully sulfonated) showed selectivities very close to those of Amberlyst 46 (only surface sulfonated); while it needed 8-fold less time to achieve a comparable level of conversion (37 min and 311 min, respectively). Therefore, among the tested acid ion-exchange resins, Dowex50Wx2 seems to be the most suitable catalyst for the synthesis of ethyl hexyl ether, whereas Amberlyst 15, perhaps the most industrially used acidic ion-exchange resin as catalyst, is definitely not a suitable one for ethyl hexyl ether production due to the poor selectivity showed.

On the selection of a suitable catalyst for ethyl hexyl ether synthesis, it is necessary that it retains its activity for long time. On that score, it has been reported that gel-type resins maintains their activity and selectivity in aqueous media for more that 80 h on stream at 393-423 K[50,51]. In particular, in the dehydration reaction between ethanol and 1-octanol to ethyl octyl ether in a fixed bed reactor, reaction rates on Dowex 50Wx2 only dropped by 10% after 70 h at 423 K[51]. Interestingly, the catalyst recovered its activity after drying in a N_2 flux and, in addition, its acid capacity was unchanged.

Taking into account that maximum operating temperature of Dowex 50Wx2 is 423 K (Table 2), if temperatures higher than 423K were needed for operation, Amberlyst 70 is a good option. It is a resin with upgraded thermal stability (T_{max} = 463K), and as selective to ethyl hexyl ether with respect to diethyl carbonate as Dowex 50Wx2 is. It is to be noted that Amberlyst 70 is as selective as gel-type resins with 2-4 DVB% in other liquid-phase dehydration reactions of alcohol to linear ether[27,34,52,53]. Moreover, in the reaction of synthesis of octyl ether in a fixed bed reactor, Amberlyst 70 was found to be reusable without activity loss after three 50 h on stream cycles, and desulfonation after 24 h at 463 K in water stream was negligible[28,51].

In relation to catalytic activity of ion-exchange resins the presence of water is outstanding. As discussed in the literature, water is essential to swell the resin making easier the access to sulfonic groups. The size of spaces formed on swelling determines selectivity to moderately bulky compounds, such as linear ethers of 8 or more carbon atoms. As a result, as seen in previous discussion, activity and selectivity to ethyl hexyl ether is higher on the more swollen resins. Kinetically, water inhibits reaction rate since it competes with the alcohol for active sites. The inhibitory effect of water on the formation of ethyl hexyl ether will be analysed in further work by performing the kinetic study. The catalytic activity decay observed in liquid-phase dehydration reaction of alcohol to ether over ion-exchange resins is ascribed to the strong competitive adsorption on acid sites, blocking the adsorption of alcohol, and to hydrolysis of the polymer backbone releasing sulphuric acid, causing desulfonation this way. Fortunately, loss of activity originated by water adsorption is fully recovered as soon as water is removed from the reaction medium[36,51].

Finally, the less selective resin Amberlyst 15, despite its maximum operating temperature is as low as 393 K, might be reused several times at 423 K without activity loss as it was shown in the dehydration of 1-butanol to di-n-butyl ether[54]. However, in this case morphology changes gaining surface area but some deactivation is detected. The maintaining of catalytic activity for a few runs would be the result of those opposite changes in the resin.

3.4 Relationship between swollen-state morphology and catalytic activity

From a chemical point of view, all acidic ion-exchange resins used in this work have a simple and uniform composition: sulfonic groups bounded to aromatic rings. Thus, the acid strength of sulfonic groups, the actual catalytic active species, was similar in most resins and only ≈5% higher in the particular case of chlorinated ones[28]. In

addition, the number of sulfonic groups was quite similar in most resins (4.8-4.95 mmol H^+/g). Despite the chemical similarity, tested catalyst showed different catalytic performances which typically are a consequence of differences in their swollen morphology[31].

In the present system, where the mixture was composed of alcohols, carbonates, ethers and water, the reaction proceeds essentially in a polar environment[21]. As a consequence, the actual working-state morphology of resins could be quite similar to that deduced from aqueous ISEC measurements discussed in section 3.1 (see Table 2). A characteristic property of acidic ion-exchange resins obtained by means of ISEC technique is V_{sp}; the more swollen resins having the higher V_{sp} values. Interestingly, recent works showed that V_{sp} values allowed to predict the catalyst performance in polar environments with high accuracy[18,34]. Likewise, it is assumed that resin V_{sp} values were able to predict their catalytic behaviour in this reaction system.

Fig. 5 shows the dependence of initial consumption-rates of reactants on V_{sp}. It is clearly seen that consumption-rate of reactants are enhanced in catalysts having high V_{sp} values. This fact could be explained because a high expanded polymer skeleton favours the accommodation of reaction intermediates and allows the access of reactants to a larger number of acid centres. In such a way, reaction rate can be increased up to 4-fold by using resins able to swell its polymer skeleton in polar environment. The differences between the consumption-rates profiles of both reactants with respect to V_{sp} are essentially due to by-products formation

According to the reaction scheme (Fig. 4), the reactions taking place at the beginning of the reaction (t=0) were essentially reactions 1, 4, 6 and 9; namely, the formation of ethyl hexyl carbonate, diethyl ether, di-n-hexyl ether and C_6 alkenes, respectively. Thus, it is assumed that the only relevant reaction that took place at t=0, not coming directly from diethyl carbonate and/or 1-hexanol, was the thermal decomposition of ethyl hexyl carbonate to ethyl hexyl ether (reaction 2), while the extent of reactions 3, 5, 7 and 8 was negligible. Accordingly, the reaction rates of product formation were calculated as follows;

$$r_1^0 = r_{EHC}^0 = \frac{1}{W_{cat}}\left(\frac{dn_{EHC}}{dt}\right)_{t=0} \quad (5)$$

$$r_4^0 = r_{DEE}^0 = \frac{1}{W_{cat}}\left(\frac{dn_{DEE}}{dt}\right)_{t=0} \quad (6)$$

$$r_6^0 = r_{DHE}^0 = \frac{1}{W_{cat}}\left(\frac{dn_{DHE}}{dt}\right)_{t=0} \quad (7)$$

$$r_9^0 = r_{alkenes}^0 = \frac{1}{W_{cat}}\left(\frac{dn_{alkenes}}{dt}\right)_{t=0} \quad (8)$$

Fig. 6 displays the influence of the V_{sp} values on products formation. Initial reaction rates of ethyl hexyl carbonate formation showed a strong dependence on the catalyst V_{sp} values, what might indicate that it is the most sterically demanding reaction. An entirely opposite behaviour was observed in the formation of alkenes as they were only detected over resins with low V_{sp} values. Therefore, the intramolecular dehydration to olefin occurred preferentially on resins with a less expanded polymer. An intermediate behaviour was observed in the formation of di-n-hexyl ether and diethyl ether, where the reaction rate dependence on V_{sp} was not relevant. This behaviour needs further discussion

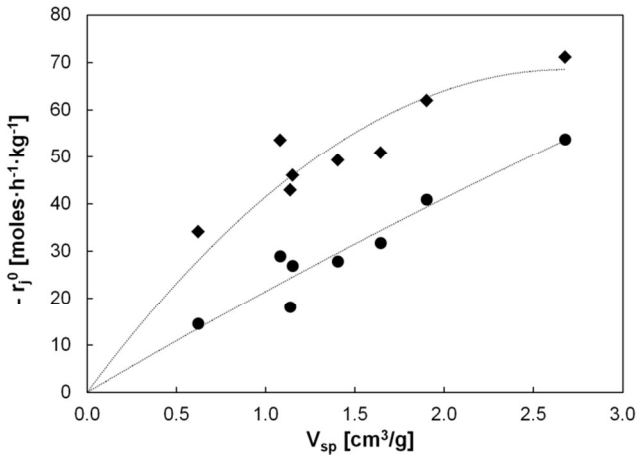

Fig. 5 Influence of the specific volume of swollen polymer (V_{sp}) on consumption-rate of reactants (● diethyl carbonate; ♦ 1-hexanol). Experimental conditions: T=423 K, P=2.5 MPa, $R_{HeOH/DEC}$=2.

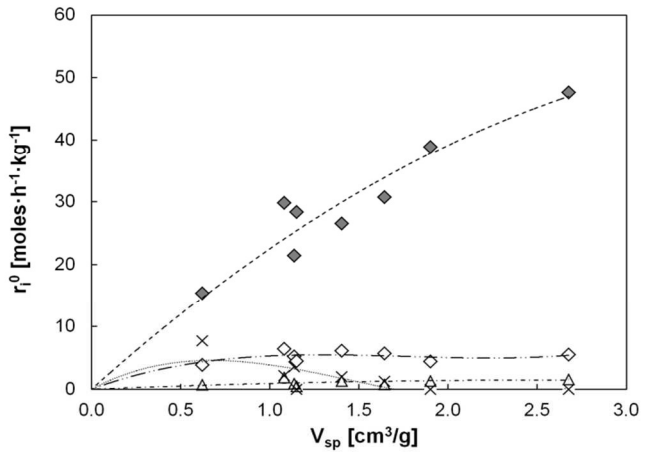

Fig. 6 Influence of the specific volume of swollen polymer (V_{sp}) on initial reaction rates of formation of compound *j* (♦ ethyl hexyl carbonate; Δ diethyl ether ◊ di-n-hexyl ether; x alkenes). Experimental conditions: T=423 K, P=2.5 MPa, $R_{HeOH/DEC}$=2.

As a consequence of the observed dependence of initial reaction rates on the V_{sp}, it might be assumed that each single reaction is favoured on different zones of the polymer, depending on the steric hindrances for reactants, products and intermediates of reaction. In this sense, the intrinsic reaction rate achieved by a catalyst can be expressed as the sum of contributions of individual polymer domains[35,42]. The individual contribution of each of the five polymer domains of a characteristic chain density was computed as follows:

$$r_i = \sum_{n=0.15}^{1.5} r_{i,n} = \sum_{n=0.15}^{1.5}\left[TOF_{i,n}^0 \times [H^+] \times \left(\frac{V_{sp,n}}{V_{sp}}\right)\right] \quad (9)$$

For a given catalyst r_i is the reaction rate of reaction *i*, $r_{i,n}$ the contribution to the reaction rate induced by polymer volume fraction *n*, $TOF_{i,n}^0$ the specific activity of polymer fraction *n* for the reaction *i* defined as reaction rate per acid site, $[H^+]$ the acid capacity, $V_{sp,n}$ the specific volume of swollen polymer occupied by fraction *n* and V_{sp} the total specific volume of swollen polymer. As only Dowex

50Wx2 shows a relevant swollen specific volume with 0.2 nm/nm^3 polymer density (see Table 2), the polymer chain concentrations of 0.1 and 0.2 nm/nm^3 were grouped as a 0.15 nm/nm^3 fraction. Then, a set of equations (r_i, one for each catalyst) and four unknown parameters ($TOF_{i,n}$, specific activity of each polymer fraction) can be obtained for each reaction. In order to obtain $TOF_{i,n}$ values, squared difference between experimental and computed values of r_i was minimized.

Distribution of the specific activity values for each polymer chain density, $TOF_{i,n}$, is depicted in Fig. 7 for species coming from diethyl carbonate. Relevant differences were observed depending on the reaction considered. The transesterification reaction of 1-hexanol with diethyl carbonate to form ethyl hexyl ether and ethanol, which is by far the most favoured reaction, showed a maximum of specific activity in the 0.4 nm/nm^3 zone. Further increase of the polymer chain density would hinder the formation of the necessary reaction intermediate due to steric limitation, and as result, polymer zones denser than 0.4 nm/nm^3 leaded to a decrease of specific activity. The most expanded zone (0.15 nm/nm^3) also showed lower specific activity since the polymer volume fraction with the lowest chain density fractions contains excessively dispersed acid groups. Tested resins contain one sulfonic group per aromatic ring of the polymer backbone, thus, the number of acid groups present in the more expandable zones was much lower.

On the contrary, the highest-performance polymer fraction for the thermal decomposition of diethyl carbonate to diethyl ether is shifted to a denser zone (0.8 nm/nm^3) showing that it is a less sterically demanding reaction. Therefore, resins containing higher volume zones of dense swollen gel-phase should be avoided as catalyst in order to favour the formation of ethyl hexyl carbonate. These results are in agreement with the lower selectivity to ethyl hexyl ether of the catalysts containing the densest zones.

As for ethyl hexyl carbonate, di-n-hexyl ether and alkenes (all formed from 1-hexanol) formation reaction, $TOF_{i,n}$ values are displayed in Fig. 8. As it is seen, the polymer zone of 0.4 nm/nm^3 density favours equally two competing reactions: the formation of ethyl hexyl carbonate and ethanol, and that of di-n-hexyl ether and water. Unfortunately, the selectivity to products formed from 1-hexanol cannot be optimized within this kind of catalysts as both reactions took place preferentially in the same polymer zone. However, the intermolecular dehydration of 1-hexanol to C_6 alkenes only takes place within the densest zone of the polymer. Thus, catalysts containing 1.5 nm/nm^3 polymer zones should be avoided.

As shown, Equation 9 provides a useful phenomenological assessment to study the catalytic behaviour at molecular level and to select a suitable catalyst depending on the desired reaction. The transesterification reaction of 1-hexanol and diethyl carbonate and the 1-hexanol intermolecular dehydration showed similar steric limitations and they occurred preferentially in medium expanded polymer zones (0.4 nm/nm^3 zone). In inorganic materials, this polymer chain density is equivalent to pores of 2.6 nm[43,44]. In contrast, the thermal decomposition of diethyl carbonate is favoured in slightly denser ones (0.8 nm/nm^3 zone, equivalent to 1.5 nm[43,44]). Finally, the formation of C_6 alkenes only takes place in zones with severe steric limitations (1.5 nm/nm^3 zone, equivalent to 1.0 nm[43,44]).

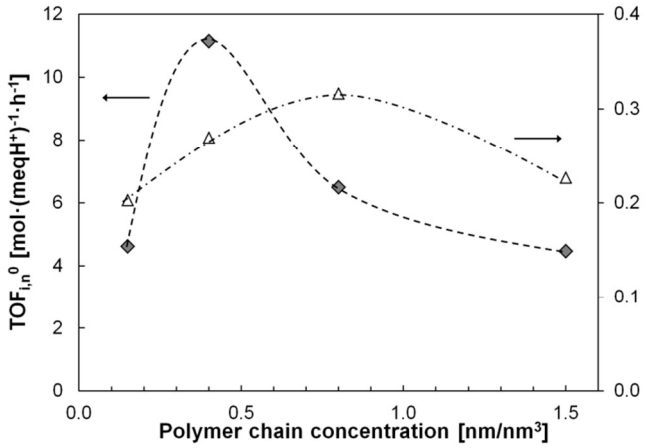

Fig. 7 $TOF_{i,n}^0$ distribution for each polymer chain density zone for the reaction *i* (♦) 1,ethyl hexyl carbonate and (Δ) 4,diethyl ether. Experimental conditions: T=423 K, P=2.5 MPa, $R_{HeOH/DEC}$=2.

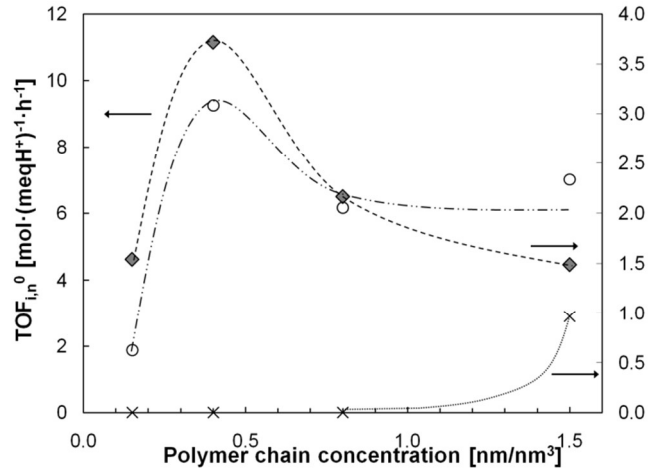

Fig. 8 $TOF_{i,n}^0$ distribution for each characteristic polymer chain density on the reaction *i* (♦) ethyl hexyl carbonate (○) di-n-hexyl ether and (x) alkenes. Experimental conditions: T=423 K, P=2.5 MPa, $R_{HeOH/DEC}$=2.

3.4 Influence of temperature on catalyst performance

The previous section revealed that the morphology of ion-exchangers is decisive to favour the transesterification reaction of diethyl carbonate with 1-hexanol and thereby enhance the further yield to ethyl hexyl ether. On the other hand, using the most suitable catalyst, a careful selection of the reaction temperature can play a key role in the process optimization. The effect of temperature were checked over the chlorinated resins Purolite CT482 and Amberlyst 70 which are thermally stable up to 463 K (see Table 2). Experiments were performed in the temperature range of 403-463K with initial molar ratio 1-hexanol to diethyl carbonate $R_{HeOH/DEC}$ = 2. The amount of catalyst was varied from 0.2 to 3.7 g to achieve a similar conversion level in the whole temperature range. Moreover, the influence of the catalyst load on reaction rate is negligible at the selected catalyst mass range[23,27,55].

Table 5. Conversion of reactants and yield to ethyl hexyl ether (P=2.5 MPa, $R_{HeOH/DEC}$=2, t=6h).

Catalyst	T(K)	W_{cat} (g)	X_{DEC} (%)	X_{HeOH} (%)	Y^{EHE}_{DEC}(%)	Y^{EHE}_{HeOH} (%)
Amberlyst 70	403	3.678 ± 0.001	49.7 ± 1.9	55.9 ± 0.3	11.0 ± 0.6	9.1 ± 0.4
	423	1.044 ± 0.001	44.8 ± 0.8	56.6 ± 0.2	12.6 ± 0.7	10.7 ± 0.5
	443	0.351 ± 0.001	42.3 ± 0.9	59.2 ± 0.2	11.3 ± 0.6	12.5 ± 0.6
	473	0.192 ± 0.001	46.1 ± 0.8	65.0 ± 0.4	19.4 ± 1.1	16.8 ± 0.4
Purolite CT482	403	3.645 ± 0.001	43.8 ± 1.4	60.2 ± 0.2	13.5 ± 0.5	7.5 ± 0.5
	423	1.061 ± 0.001	53.9 ± 1.8	57.8 ± 0.2	17.3 ± 0.6	15.1 ± 0.8
	443	0.353 ± 0.001	51.0 ± 1.9	61.0 ± 0.2	18.8 ± 0.5	16.6 ± 0.7
	473	0.193 ± 0.001	62.7 ± 1.3	62.7 ± 0.2	26.6 ± 0.9	21.5 ± 1.2

Table 6. Estimated selectivity at the conversion level of X_{DEC}=10% over Amberlyst 70 (P=2.5 MPa, $R_{HeOH/DEC}$=2)

T (K)	W_{cat} (g)	X_{HeOH} (%)	S^{EHC}_{DEC} (%)	S^{DEE}_{DEC} (%)	S^{EHC}_{HeOH} (%)	S^{DHE}_{HeOH} (%)	$S^{alkenes}_{HeOH}$ (%)
403	3.678 ± 0.001	20.4 ± 3.5	97.6 ± 0.8	2.4 ± 1.2	76.3 ± 0.5	23.1 ± 0.2	0.2 ± 0.2
423	1.044 ± 0.001	22.6 ± 0.4	96.2 ± 2.4	3.8 ± 2.4	64.6 ± 1.2	35.7 ± 0.5	0.6 ± 0.6
443	0.351 ± 0.001	24.1 ± 0.1	91.7 ± 5.1	8.3 ±0.7	52.4 ± 0.4	45.5 ± 0.4	2.6 ± 0.1
463	0.192 ± 0.001	24.4 ±2.0	90.9 ± 2.9	9.6 ± 3.7	44.4 ± 0.1	50.1 ± 0.6	5.7 ± 0.4

As seen in Table 5, despite changing the catalyst mass on increasing the working temperature, conversion levels in the range 42 -50 % over Amberlyst 70 and 43–63 % over Purolite CT482 for X_{DEC}, and 55-65% over Amberlyst 70 and 57-63% over Purolite CT482 for X_{HeOH}, makes difficult to clearly evaluate the influence of temperature. As a whole, data show a high dependence on temperature since about the same conversion level is obtained on increasing temperature 20 K by decreasing the catalyst mass to a third. It is to be noted that the yield of ethyl hexyl ether with respect to both diethyl carbonate and 1- hexanol also increases with temperature, what could be because reaction rate of decomposition of ethyl hexyl carbonate to ethyl hexyl ether is highly increased with temperature.

To see the effect of temperature on selectivity, Table 6 shows X_{HeOH} and selectivity over Amberlyst 70 at each temperature at X_{DEC} = 10%. As seen, 1-hexanol conversions increases slightly what points out that side reactions of formation of di-n-hexyl ether and olefins accelerates with temperature more than reaction of transeserification to ethyl hexyl carbonate. As a whole, selectivity to diethyl ether from diethyl carbonate and selectivity to di-n-hexyl ether and olefins from 1-hexanol increases with temperature. As a consequence, the ability to obtain ethyl hexyl ether decreases with temperature as shown by the selectivity to ethyl hexyl carbonate with respect to diethyl carbonate (91% < S^{EHC}_{DEC} < 98%) or with respect to 1-hexanol (44 %< S^{EHC}_{HeOH} < 77%). Again, it is to be noted that at this low conversions levels a small quantity of ethyl hexyl ether is also formed.

Apparent activation energies of the four competitive reactions at low conversion level were obtained from Arrhenius plots of initial reaction rates. Fig. 9 shows the Arrhenius plot for Purolite CT482. As seen the plot displays very good straight lines what indicates that the rate limiting step do not changes over the temperature range explored. Arrhenius plot for initial reaction rates on Amberlyst 70 show a similar trend. Apparent activation energies found from the slope of Arrhenius plots are shown in Table 7.

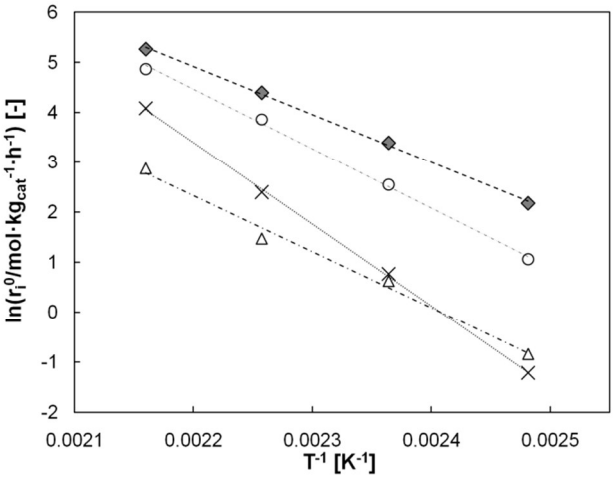

Fig. 9 Arrhenius plot of initial reaction rates of reaction *i* on CT482. (♦ ethyl hexyl carbonate; Δ diethyl ether formation; ○ di-n-hexyl ether formation; x alkenes formation). Experimental conditions: P=2.5 MPa, $R_{HeOH/DEC}$=2.

Table 7. Apparent activation energies on thermal stable acid ion-exchange resins at $R_{HeOH/DEC}$ =2

E_a(kJ/mol) / Catalyst	EHC	EHE	DEE	DHE	Alkenes
Amberlyst 70	68 ± 3	98 ± 3	103 ± 13	102 ± 4	143 ± 18
Purolite CT482	78 ± 1	100 ± 6	98 ± 6	101 ± 4	136 ± 4

Apparent activation energies for linear ether formation are in total agreement with those previously reported for diethyl ether and di-n-hexyl ether formation on Amberlyst 70 by means of intermolecular dehydration of ethanol (Ea_{DEE}=100 ± 5 kJ/mol)[36] and 1-hexanol (Ea_{DHE}=108 ± 7 kJ/mol)[52], respectively. On the other hand, apparent

activation energy for ethyl hexyl ether synthesis is similar to that one found for ethyl octyl ether over Amberlyst 70 (E_a = 105 ± 4 kJ/mol)[36]. Finally, apparent energies for linear ether formation over Amberlyst 70 are also similar to those of dehydration of 1-pentanol to di-n-pentyl ether (118.7 ± 0.2 kJ/mol)[57] and that of 1-octanol to di-n-octyl ether from (114 ± 7 kJ/mol)[58], respectively. Since in all quoted studies it was experimentally checked that resistance to external mass transfer and diffusion was negligible, it can be assumed that reported data in the present work are free of mass transfer effects.

As seen in Table 7, the lowest temperature dependence was observed on the desired transesterification of diethyl carbonate to ethyl hexyl carbonate (Ea_{EHC}=68-78 kJ/mol) whereas the highest dependence was found on the side reaction of intramolecular dehydration to C_6 alkenes ($Ea_{alkenes}$=136-143 kJ/mol). Ethers formation reactions showed intermediate temperature dependencies ($Ea_{EHE} \approx Ea_{DEE} \approx Ea_{DHE} \approx$ 98-103 kJ/mol). These apparent activation energy values are in line with literature which shows that in the dehydration of C_5-C_{12} linear alcohols, olefin formation is favoured at high temperatures but that of linear ether is favoured at low temperature[12]. Accordingly, activation energy for alcohol dehydration to olefin is higher than that of linear ether formation. On the other side, transesterification reactions are much less sensitive to temperature as it is also shown in the transesterification of ethyl acetate with methanol on several ion-exchange resins (48-52 kJ/mol)[32].

On a technical standpoint, given that the formation of different type of compounds (carbonates, ethers and alkenes) showed different activation energy values, an important task in order to implement an industrial process for obtaining ethyl hexyl ether by reaction between diethyl carbonate and 1-hexanol is the selection of working temperature range. This is essential to produce readily and selectively ethyl hexyl ether, as data of Table 6 shows, since an increase of temperature enhances reaction rate but decrease selectivity to ethyl hexyl ether. This behaviour agrees with the fact that activation energy values for ether formation are intermediate between those of trans-esterification to ethyl hexyl carbonate and dehydration to olefin. Since in industry, selectivity has priority over conversion, it follows that it is preferable working at low temperature. A relevant drawback of conduct the reaction at low temperature would be the requirement of higher amount of catalyst and/or longer reaction time (or reactor volume, in continuous processes). However, energy savings brought about by working at low temperature is a very important benefit to take into account.

A possible reactor design might use two units reactor connected in series. According to estimated activation energy values, the selectivity to ethyl hexyl carbonate is clearly favoured at low temperatures. On the contrary, ethyl hexyl ether, diethyl ether and di-n-hexyl ether syntheses are favoured at intermediate temperature, whereas alkenes formation is favoured at higher ones. The first reactor should operate at low temperature increasing this way the selectivity to ethyl hexyl carbonate and hindering the production of byproducts (di-n-hexyl ether, diethyl ether and olefins). The second unit would work at higher temperature than the first one to increase the reaction rate of thermal decomposition of ethyl hexyl carbonate into ethyl hexyl ether. Nevertheless, further research is necessary to implement such two-reactor unit.

4. Conclusions

Ethyl hexyl ether can be successfully formed using diethyl carbonate and 1-hexanol over acidic ion-exchange resins by means of two reaction pathways: thermal decomposition of ethyl hexyl carbonate and intermolecular dehydration of ethanol with 1-hexanol. Nevertheless, both routes require previously the transesterification step of diethyl carbonate with 1-hexanol giving place to ethyl hexyl reaction pathways: thermal decomposition of ethyl hexyl carbonate and intermolecular dehydration of ethanol with 1-hexanol. This reaction is favoured in gel-phase zones of 0.4 nm/m^3 chains polymer density (equivalent to 2.6 nm diameter pores). Unfortunately, the main by-product, di-n-hexyl ether, is also preferentially formed in polymer zones of the same density. Therefore, it would be significantly formed together with ethyl hexyl ether. However, both ethers are excellent diesel additives and they can be introduced to the diesel pool jointly without further separation.

On the contrary, the thermal decomposition of diethyl carbonate is favoured in slightly denser polymer zones (0.8 nm/nm^3) and the formation of C_6 alkenes only takes place in zones with severe steric limitations (1.5 nm/nm^3 zone). Both products are less desired as diesel additives. Thus, the synthesis of ethyl hexyl ether should be carried out on polymers with medium to low dense polymer fractions. To the best of our knowledge, ion-exchange resins with swollen gel-phase with only a zone of low polymer density are not currently available. Therefore, acid ion-exchangers with a high swollen volume fraction of 0.4 nm/nm^3 polymer density are selected for industrial production, *e.g.* Dowex 50Wx2 or Amberlyst 70.

Finally, a decrease of the reaction temperature would favour the reaction between 1-hexanol and diethyl ether to ethyl hexyl ether as showed lower temperature dependence (Ea_{EHC}=67-80 kJ/mol), while all the non-desired reactions showed higher temperature dependence (Ea=91-136 kJ/mol). This fact would be useful for designing the reactor unit of a potential industrial process to upgrade the selectivity to ethyl hexyl carbonate and further, that of ethyl hexyl carbonate decomposition to ethyl hexyl ether.

Acknowledgements

Financial support was provided by the Science and Education Ministry of Spain (project: CTQ2010-16047). The authors thank Rohm and Haas France and Purolite for providing Amberlyst and CT ion-exchange resins, respectively. Finally, the authors would like to express their gratefulness to Dr. Karel Jerabek of Institute of Chemical process Fundamentals (Prague, Czech Republic) for discussing the ISEC analyses.

Nomenclature

$[H^+]$	acid capacity (mmol $H^+ \cdot g_{cat}^{-1}$)
DEC	diethyl carbonate
DEE	diethyl ether
DHE	di-n-hexyl ether
d_p	particle diameter (mm)
E_a	apparent activation energy (kJ·mol^{-1})
DVB	divinylbenzene
EHC	ethyl hexyl carbonate
EHE	ethyl hexyl ether
HeOH	1-hexanol
ISEC	inverse steric exclusion chromatography
i	reaction
j	reactant
k	product
n	gel-resin zone characterized by a given chains density
n_j	number of moles of compound j (mol)
P	pressure (MPa)
R	molar ratio (mol/mol)

$r_{i,n}$	contribution to the reaction rate *i* induced by polymer fraction *n* ($mol \cdot k_{gcat}^{-1} \cdot h^{-1}$)
r_j^0	rate of formation of compound j ($mol \cdot kg_{cat}^{-1} \cdot h^{-1}$)
r_i	reaction rate of reaction *i* ($mol \cdot kg_{cat}^{-1} \cdot h^{-1}$)
S_j^k	selectivity to *k* with respect to reactant *j* (mol %)
t	time (h)
T	temperature (K)
T_{max}	maximum operating temperature (K)
$TOF_{i,n}^0$	the specific activity of the polymer fraction *n* for the reaction *I* ($mol \cdot (meq\ H^+)^{-1} \cdot h^{-1}$)
V_{sp}	specific volume of swollen polymer (cm^3/g)
$V_{sp,n}$	specific volume of swollen polymer occupied by fraction *n* (cm^3/g)
W_{cat}	mass of dry catalyst (g)
X_j	conversion of compound *j* (mol. %)
Y_j^{EHE}	yield of ethyl hexyl ether with respect to reactant *j* (mol. %)
$[H^+]$	acid capacity ($mmol\ H^+ \cdot g^{-1}$)

References

1 S. Salvi, A. Blomerg, B. Rudell, F. Kelly, T. Sandstrom, S. T. Holgate, and A. Frew, *Am. J. Respir. Crit. Care Med.*, 1999, **159**, 702–709.

2 R. O. McClellan, *Annu. Rev. Pharmacol. Toxicol.*, 1987, **27**, 279–300.

3 J. Kagawa, *Toxicology*, 2002, **181-182**, 349–353.

4 M. Riedl and D. Diaz-Sanchez, *J. Allergy Clin. Immunol.*, 2005, **115**, 221–228.

5 S. H. L. Yim and S. R. H. Barrett, *Environ. Sci. Technol.*, 2012, **46**, 4291–4296.

6 F. Liotta and D. Montalvo, *SAE Tech. Pap.*, 1993, **932734**

7 C. Y. Choi and R. D. Reitz, *Fuel*, 1999, **78**, 1303–1317.

8 C. C. Barrios, C. Martín, A. Domínguez-Sáez, P. Álvarez, M. Pujadas, and J. Casanova, *Fuel*, 2014, **132**, 93–100.

9 *E-diesel (oxygenated diesel),* http://www.oxydiesel.com, 2014.

10 B. G. Harvey and H. A. Meylemans, *J. Chem. Technol. Biotechnol.*, 2011, **86**, 2–9.

11 B. Martin, P. Aakko, D. Beckman, and N. Del Giacomo, *SAE Tech. Pap.*, 1997, **972966**.

12 R. J. J. Nel and A. de Klerk, *Ind. Eng. Chem. Res.*, 2009, **48**, 5230–5238.

13 D. C. Rakopoulos, C. D. Rakopoulos, E. G. Giakoumis, and A. M. Dimaratos, Energy, 2012, 43, 214–224.

14 B. Bailey, J. Eberhardt, S. Goguen, and J. Erwin, *SAE Tech. Pap.*, 1997, **972978**.

15 İ. Sezer, *Int. J. Therm. Sci.*, 2011, **50**, 1594–1603.

16 K. Górski and M. Przedlacki, *Energy & Fuels*, 2014, **28**, 2608–2616.

17 M. Karabektas, G. Ergen, and M. Hosoz, *Fuel*, 2014, **115**, 855–860.

18 R. Bringué, E. Ramírez, M. Iborra, J. Tejero, and F. Cunill, *J. Catal.*, 2013, **304**, 7–21.

19 G. Olah, US Patent 5,520,710, 1996.

20 A. J. Parrott, R. A. Bourne, P. N. Gooden, H. S. Bevinakatti, M. Poliakoff, and D. J. Irvine, *Org. Process Res. Dev.*, 2010, **14**, 1420–1426.

21 J. Guilera, R. Bringué, E. Ramírez, M. Iborra, and J. Tejero, *Ind. Eng. Chem. Res.*, 2012, **51**, 16525–16530.

22 P. Tundo, S. Memoli, D. Herault, and K. Hill, *Green Chem.*, 2004, **6**, 609–612.

23 R. Bringué, E. Ramírez, M. Iborra, J. Tejero, and F. Cunill, *Chem. Eng. J.*, 2014, **246**, 71–78.

24 X. Gao, A. Krzywicki, D. S, R. Johnston, and A. Kalivoda, US Patent 7,576,250, 2009.

25 R. Bringué, J. Tejero, M. Iborra, C. Fité, J. F. Izquierdo, and F. Cunill, *J. Chem. Eng. Data*, 2008, **53**, 2854–2860.

26 M. A. Harmer and Q. Sun, *Appl. Catal. A Gen.*, 2001, **221**, 45–62.

27 R. Bringué, M. Iborra, J. Tejero, J. F. Izquierdo, F. Cunill, C. Fité, and V. Cruz, *J. Catal.*, 2006, **244**, 33–42.

28 P. F. Siril, H. E. Cross, and D. R. Brown, *J. Mol. Catal. A Chem.*, 2008, **279**, 63–68.

29 S. Koujout and D. R. Brown, *Thermochim. Acta*, 2005, **434**, 158–164.

30 J.-A. Dalmon and G. A. Martin, *J. Chem. Soc. Faraday Trans.*, 1979, **75**, 1011–1015.

31 K. Jerabek, *Kem. u Ind.*, 2013, **62**, 171–176.

32 E. Van de Steene, J. De Clercq, and J. W. Thybaut, *Chem. Eng. J.*, 2014, **242**, 170–179.

33 Y. Bing, C. Hailin, Y. Hua, L. Xuesong, J. Mingming, and D. Wang, *J. Nanosci. Nanotechnol.*, 2014, **14**, 1790–1798.

34 J. Guilera, R. Bringué, E. Ramírez, M. Iborra, and J. Tejero, *Appl. Catal. A Gen.*, 2012, **413-414**, 21–29.

35. J. H. Badia, C. Fité, R. Bringué, M. Iborra, and F. Cunill, *16th Nord. Symp. Catal.*, 2014.

36 J. Guilera, R. Bringué, E. Ramírez, C. Fité, and J. Tejero, *AIChE J.*, 2014, **60**, 2918–2928.

37 A.G. Ogston, *Trans. Faraday Soc.* 54 (1958) 1754

38 K. Jerábek and K. Setínek, *J. Polym. Sci. Part A Polym. Chem.*, 1990, **28**, 1387–1395.

39 Y. Yao and A. M. Lenhoff, *J. Chromatogr. A*, 2004, **1037**, 273–282.

40 A. A. D'Archivi, L. Galantini, A. Panatta, E. Tettamanti, and B. Corain, *J. Phys. Chem. B*, 1998, **102**, 6774–6779.

41 I. Bacskay, A. Sepsey, and A. Felinger, *J. Chromatogr. A*, 2014, **1339**, 110–7.

42 K. Jerabek, *ACS Symposium Series*, 635 (1996) 211-224.

43 K. Jerabek, L. Holub, in 13th International IUPAC Conference on Polymers and Organic Chemistry, Montreal, 2009

44 S. Sterchele, P. Centomo, M. Zecca, L. Hanková, and K. Jeřábek, *Microporous Mesoporous Mater.*, 2014, **185**, 26–29.

45 Z. Zhang, Q. Wang, P. Tripathi, and C. U. Pittman Jr, *Green Chem.*, 2011, **13**, 940–949.

46 I. Dosuna-Rodríguez and E. M. Gaigneaux, *Catal. Today*, 2012, **195**, 14–21.

47 L. Rios, D. Echeverri, and F. Cardeño, *Ind. Crops Prod.*, 2013, **43**, 183–187.

48 W. Schutyser, S.-F. Koelewijn, M. Dusselier, S. de Vyver, J. Thomas, F. Yu, M. J. Carbone, M. Smet, P. Van Puyvelde, W. Dehaen, and B. F. Sels, *Green Chem.*, 2014, **16**, 1999–2007.

49 P. Barbaro and C. M. Marrodan, *Green Chem.*, 2014, **16**, 3434–3438.

50 L. Petrus, E.J. Stamhuis, G.E.H. Josteen, *Ind. Eng. Chem, Proc. Res. Dev.* 1981, **20** 366-371

51 J. Guilera, E. Ramírez, C. Fité, M. Iborra, and J. Tejero, *Appl. Catal. A Gen.*, 2013, **467**, 301–309.

52 E. Medina, R. Bringué, J. Tejero, M. Iborra, and C. Fité, *Appl. Catal. A Gen.*, 2010, **374**, 41–47.
53 C. Casas, R. Bringué, E. Ramírez, M. Iborra, J. Tejero, *Appl. Catal. A: Gen*. 2011, **396**, 129-139
54 M.A. Pérez, R. Bringué, M. Iborra, J. Tejero, F. Cunill, *Appl. Catal. A: Gen:* 2014, **482**, 38-48
55 M. Granollers, J. F. Izquierdo, J. Tejero, M. Iborra, C. Fité, R. Bringué, and F. Cunill, *Ind. Eng. Chem. Res.*, 2010, **49**, 3561–3570
56 R. Bringué, E. Ramírez, C. Fité, M. Iborra, J. Tejero, *Ind. Eng. Chem. Res*. 2011, **50**, 7911-7919
57 C. Casas, Ph. D. Thesis, University of Barcelona, 2013.

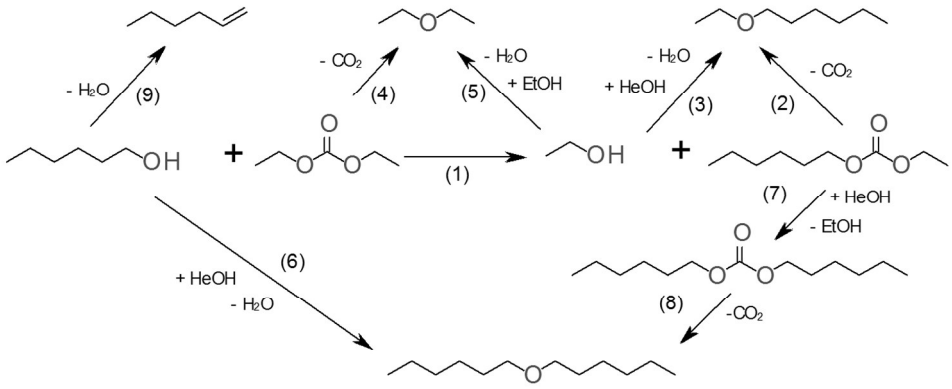

Identifying the resin polymer zones where ethyl hexyl ether and byproducts are preferentially formed in hexanol etherification with diethyl carbonate
321x132mm (120 x 120 DPI)